ISSN NO. 2320-5407

Journal homepage: http://www.journalijar.com
Journal DOI: 10.21474/IJAR01

INTERNATIONAL JOURNAL OF ADVANCED RESEARCH

RESEARCH ARTICLE

FABRICATION AND ANALYSIS OF THE EFFECT OF DOPING TIO_2 IN 1393 BIOACTIVE GLASS.

***Sandeep Kumar Yadav, Vikash Kumar Vyas, Sunil Prasad and Ram Pyare.**
Department of Ceramic Engineering. Indian Institute of Technology (Banaras Hindu University) Varanasi -221005, India.

Manuscript Info

Manuscript History:

Received: 18 May 2016
Final Accepted: 23 June 2016
Published Online: July 2016

Key words:
1393 Bioactive glass, titanium oxide, FTIR Spectrometry, SEM and Mechanical properties.

Corresponding Author

Sandeep Kumar Yadav

Abstract

From the previous studies on bioactive glasses it was suggested that assimilating small quantities of TiO_2 may result in an increase in the bioactivity and hydroxyapatite formation. Titanium is present in several inert biomaterials such as hip prosthesis made of titanium, screws and plates to repair bone damages. It does not induce an inflammatory response because it is a good biocompatible material. It is also used in the materials for aerospace because it has good mechanical properties. It allows reinforcing biomaterials.1393 Bioactive Glass in addition to TiO_2 (x=0-2.5%) was prepared by melting quenching technique, the present work explores the effects of titanium oxide additions. Bioactivity of the glass samples was assessed through their hydroxyapatite formation ability by immersing them in the simulated body fluid (SBF) for different soaking periods. The formation of hydroxyapatite was confirmed by FTIR spectrometry, pH measurement and microstructure evaluation through Scanning Electron Microscopy (SEM). Densities and mechanical properties of the samples were found to increase considerably with an increase in the concentration of titanium oxide.

Introduction:-

Bioactive glasses are of importance for biomedical applications due to their ability to chemically bond to bone and stimulate new bone growth (Liu et al., 1994), good mechanical stability (Hench et al., 1991) and making free from disease (Buck et al., 1989 and Hench et al., 1993). Under physiological conditions bioactive glasses liquefy in a controlled manner releasing calcium and phosphorous into solution (Hench et al., 2006). Ca and P form a non crystalline calcium phosphate layer (ACP) which then crystallizes to form hydroxyapatite (HA) / Hydroxyl-carbonate apatite (HCA): the naturally occurring mineral present in both teeth and bones (L.L. Hench and O. Andersson, 1993 and Splinter et al., 1971).

Recent developments in tissue engineering in the field of orthopedic implants look forward to developing the regeneration capabilities of the host tissues using most recent designing methods for research of implants to match the structure of the host tissues in order to accelerate the rejuvenation of the dead tissues (K. Franks and I. Abrahams, 2001; V. Patricia and M.P. Marinade, 2004; Oana Bretcanu et al., (2009); Fathi and Hanifi, 2007; Kansal and Goel, 2011). This requires the preparation of implants which are similar to that of the host tissue structure both in terms of arrangement as well as mechanical and biological properties (Kokubo and Kim, 2003; Shim and Wechsler, 1996; Watts and Hill, 2010; Rezwan and Blaker, 2006; Austin and Smith, 2013). In reference to the more than requirements, bioactive glasses have shown capable prospects. Due to their class a bioactivity showing both osteoconduction and osteoproduction, have become the material of major interest. Since the revolutionizing paper by Hench on bioactive glass in the 70s, the composition has been optimized several times for better results than the last one (Kaur and Sharma, 2012; Leenakul and Kantha, 2013; Vogal et al., 1969; Kokubo and Takadama, 2006; Sooksaen and Suttiruengwong, 2008). Glasses are composed of network forming, modifying and intermediate oxides. They present a non crystalline character reflecting structural disarray. Metal elements introduced in the glass

matrix may involve specific changes in thermal behavior (Bretcanu et al., 2009). In the glassy matrix, if there are no enough alkaline ions, the intermediate element will be a network modifier by creating two oxygen bridges (Peitl Filho et al., 1996 and Zanotto et al., 2000). Conversely, if there are enough alkaline ions, the intermediate element will be a network former. Studies have shown the impact of titanium on the thermal properties (Clark et al., 1989 and Azooz et al., 2003). Numerous researches about borophosphate glasses have shown the effect of the addition of TiO_2 on their heat treatment characteristics. The results showed a non-linear change of glass transition temperature (Gayathri Devi et al., 2010).

In the present investigation, an attempt has been made to study the effect of titanium oxide doping in base 1393 bioactive glasses to find its bioactivity and mechanical behavior.

Material and Methods:-

Selection of composition and preparation of the bioactive glass:-

The bioactive glass composition was formulated from K_2O-MgO-Na_2O-CaO-SiO_2-P_2O_5glass system. Proposed bioactive glasses containing chemical composition (53-X) SiO_2-6Na_2O- 20CaO-4 P_2O_5-12K_2O-5MgO+XTiO_2 (Where X=0-2 gram of titanium oxide) was prepared. In the present study the CaO, Na_2O, MgO, K_2O and P_2O_5 concentration was kept constant and SiO_2 was partially replaced with titanium oxide. The compositions of prepared bioactive glasses are given in Table-1.The bioactive base glass and titanium oxide doped glass was prepared by addition of titanium oxide (0-2 gram) in place of SiO_2 using the normal melting and annealing technique. Materials used include fine-grained quartz for silica. Lime and soda were introduced in the form of their respective anhydrous carbonates; potassium carbonate for K_2O, anhydrous magnesium carbonate was used as the source of MgO. P_2O_5 was added in the form of ammonium dihydrogen phosphate. The weighed batches were mixed thoroughly for 30 minutes and melted in a 100 ml platinum crucibles to get the desired bioactive glass composition as given in Table-1. The melting was carried out in an electric furnace at 1400±10°C for 2 hours in the air as furnace atmosphere and homogenized melts were poured on the preheated aluminum sheet. The prepared bioactive glass samples were directly transferred to a regulated muffle furnace at 480^{o}C for annealing. After 1 hour of annealing the muffle furnace was cooled to room temperature with controlled rate of cooling at 20°C per min.

Table 1:- Composition of Bioactive Glass (wt %)

	SiO_2	Na_2O	CaO	P_2O_5	TiO_2	K_2O	MgO
1393	53.00	6.00	20.00	4.00	0.00	12.00	5.00
TiO_2-1	52.50	6.00	20.00	4.00	0.50	12.00	5.00
TiO_2-2	52.00	6.00	20.00	4.00	1.00	12.00	5.00
TiO_2-3	51.50	6.00	20.00	4.00	1.50	12.00	5.00
TiO_2-4	51.00	6.00	20.00	4.00	2.00	12.00	5.00

Preparation of SBF:-

Kokubo and his colleagues developed a simulated body fluid that has inorganic ion concentrations similar to those of human body fluid in order to reproduce in vitro formation of apatite on bioactive materials (Kokubo T and Takadama H., 2006). The SBF solution was prepared by dissolving reagent-grade NaCl, KCl, $NaHCO_3$, $MgCl_2.6H_2O$, $CaCl_2$ and KH_2PO_4 into double distilled water and it was buffered at pH=7.4 with TRIS (trishydroxymethyl amino methane) and 1N HCl at 37 °C as compared to the human blood plasma (WBC). The ion concentrations of SBF are given in the Table-2 (Kokubo T and Takadama H., 2006).

Table 2:- Ion concentration (mM/litre) of simulated body fluid and human blood plasma

Ion	Na^+	K^+	Mg^{2+}	Ca^{2+}	HCO_3^-	HPO_4^-	SO_4^{2-}	Cl^-
Simulated body fluid	142.0	5.0	1.5	2.5	4.2	1.0	0.5	147.8
Human blood plasma	140.0	5.0	1.5	2.5	27.0	1.0	0.5	103.0

Powder X-ray diffraction (XRD) measurements:-

The bioactive glass samples were ground to 75 microns and the fine powders were subjected to X-ray diffraction analysis (XRD) using RIGAKU-Miniflex II diffractometer adopted Cu-Kα radiation (λ = 1.5405A°) with a tube voltage of 40 KV and current of 35mA in a 2θ range between 20^{o} and 80^{o}. The step size and measuring speed was set to 0.02° and 1° per min, respectively, was used in the present investigation. The JCPDS-International Centre for diffraction Data Cards were used as a reference.

Structural analysis by FTIR Reflectance spectrometry:-
The structure of bioactive glass was measured at room in the frequency range of 4000–400 cm^{-1} using a Fourier transform infrared spectrometer, (VARIAN scimitar 1000, USA). The fine bioactive glass powder samples were mixed with KBr in the ratio of 1:100 and the mixtures were subjected to an evocable die at a load of 10 bar pressure to produce clear homogeneous discs. The prepared discs were immediately subjected to IR spectrometer to measure the reflectance spectra in order to avoid moisture attack.

In vitro bioactivity study of bioactive glass:-
In order to investigate the formation of (calcium phosphate) apatite layer on the surface of the samples after immersion in SBF solution. The sample (2g) was immersed in 20 ml of SBF solution in a small plastic container at 37 $^{\circ}$C with pH 7.40 in an incubator at the static condition for the following time period 1, 3,7,15 and 30 days. After soaking, the samples were filtered, rinsed with doubly distilled water, and dried in an oven at 100 ºC for 2 hours before analysis by FTIR and SEM.

Mechanical Behavior Measurements:-
The melting were cast in the rectangular shape mould and the resulting bioactive glass samples were ground and polished for required dimension using a grinding machine then samples were subjected to three point bending test. The test was performed at room temperature using Instron Universal Testing Machine (AGS 10kND, SHIMADZU) of cross-head speed of 0.5 mm/min and full scale load of 2500 kg. Flexural strength was determined according to ASTM Standard: C158-02(2012). Using polished bioactive glass samples and the hardness testing machine the size of sample were 10mm x 10mm x 10 mm according to ASTM Standard: C730-98. The indentations have been made for loads ranging between 30 mN and 2000 mN, applied at a velocity of 1 mm/s and allowed to equilibrate for 16 second before measurement. The densities of casted bioactive glasses were measured by Archimedes principle with water as the immersion fluid. The measurements were performed at room temperature. Thin copper wire was used for immersing the samples into water. The density was determined by using ASTM: B962-14.Compressive strength of the bioactive glass samples having size of 2 x 2 x 1 cm^{-1} dimension according to ASTM D3171 were subjected to compression test. The test was performed using Instron Universal Testing Machine at room temperature (cross speed of 0.05 cm/min and full scale of 5000 kgf).

pH measurement:-
The pH of 1393 bioactive glass powder (2 g) was soaked in 20 ml of SBF solution at 37 $^{\circ}$C for different time period and the pH was measured using Universal Bio microprocessor pH meter. The instrument was calibrated each time with standard buffer solutions of pH 4.00 and 7.00 at room temperature and pH values have been recorded during different time periods at a fixed time interval.

Surface morphology (SEM):-
The SEM of 1393 bioactive glass powders (1 g) were pressed (load of 10 MPa) into pellet form using an evocable die to produce discs of 10 mm in dia. The pellets were immersed in SBF (10 ml) for 7 days at 37 ^{o}C the surface orphology of samples was analyzed before and after SBF treatment using a scanning electron microscope (SEM - Inspect S50, FEI). The samples were coated with gold (Au) by sputter coating instrument before analyzing SEM.

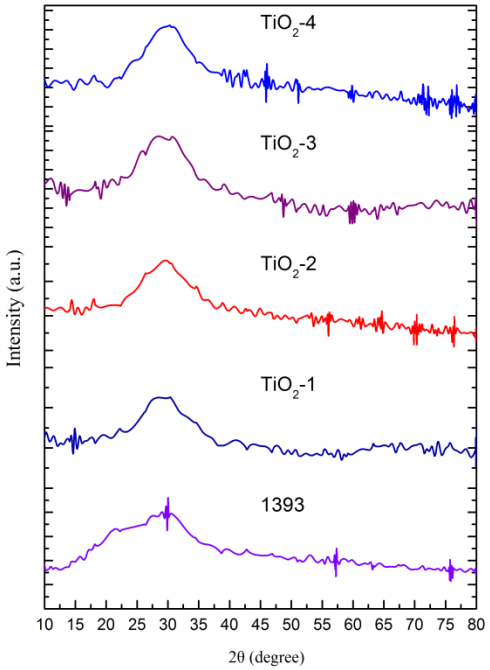

Fig 1:- X-RD bioactive glass.

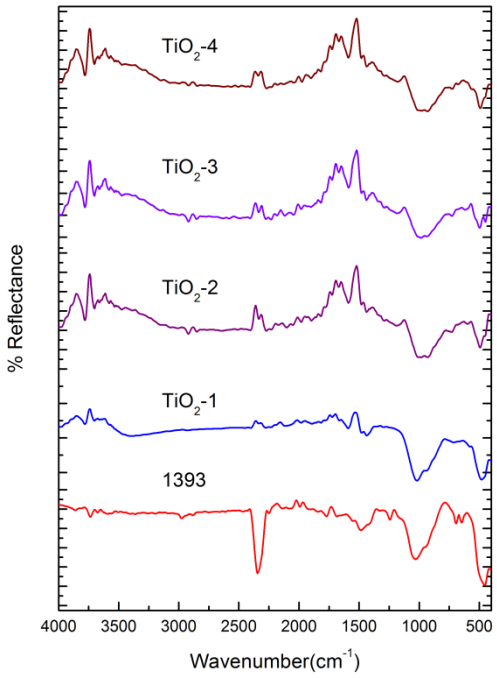

Fig 2:- FTIR before SBF.

Results and discussion:-

Structural analysis of bioactive glass:-

The X-Ray diffraction (X-RD) patterns for 1393 bioactive glass and titanium oxide doped 1393 bioactive glasses are shown in **Fig:-1**. The observed result indicates that the glasses have amorphous structure and there is no indention for the presence of crystalline phases. It was observed that the concentration titanium oxide increase in the composition the broad hump at 2θ between 25° to 35° become more intense. This may be due to the Ti^{2+} expanding the silica network (Rajendran et al., 2010)

Fig:-2 shows the FTIR Reflection spectra of the 1393 and titanium oxide doped bioactive glass before SBF treatment. All the bioactive glass samples are showing similar trend behavior, FTIR Reflection spectra bands of all the glasses confirm the main characteristic of silicate network and this may be due to the presence of SiO_2 as a major constituent. Therefore, the bioactive glass (TiO_2-1) shows the peaks 470, 722, 1022, 1430 and 3775 cm^{-1}. The resultant IR spectra at 470 cm^{-1} associated with a Si–O-Si symmetric bending mode, the band at 722 cm^{-1} corresponds with Si–O–Si symmetric stretch of non-bridging oxygen atoms between tetrahedral. It was observed that the intensity of the band recreated as the titanium oxide substitution in the 1393 bioactive glasses, therefore the titanium oxide increases the non bridging oxygen in the network. The major band at about 1022 cm^{-1} can be attributed to Si-O-Si stretching. The small band at 1430 cm^{-1} attributed to C–O vibration mode. It was noticed that the intensity of the IR peak increased as the concentration of titanium oxide increase, which is due to the breaking of Si-O-Si network. The small, broad band centered at about 3775 cm^{-1} can be assigned to the hydroxyl group (–OH) which may be the presence of adsorbed water molecules. This is shows in depicts the infrared frequencies and related functional structural groups in the bioactive glass (Nayak et al., 2010). The bioactive glasses substituted with titanium oxide are not showing noticeable changes in the IR spectra bands.

pH behavior in SBF :-

The variation in pH values of simulated body fluid (SBF) after soaking of 1393 bioactive glasses for various time periods is shown in **Fig:- 3**. It was observed that the pH of all samples shows the similar trend of behavior (Marta Cerrutia et al., 2005).The maximum pH values were recorded on 3 days of immersion. It is interesting to note that the Ti-doped bioactive glasses demonstrated a higher pH value after immersion in SBF which is due to the fast release of cations from the level surface compared with 1393 bioactive glass sample. It was observed that due to the addition of titanium oxide in base bioactive glass (1393). The sequence of reactions occurred in the SBF different day immersion of bioactive glasses for various time periods are in favor of formation of hydroxyl apatite like layer

on the surface of the samples (Hench et al., 1998; Cortes et al., 1999 and Qiu et al., 1999).In general higher is the degradation higher would be the bioactive .Therefore the titanium oxide doped glasses expected to be high bioactive. The samples No's TiO_2-1, TiO_2-2 (wt %) were revealed highest pH among the others. The TiO_2-1 and TiO_2-2 contains 0.50 & 1.00 (wt %) of titanium oxide possessed higher pH and on further addition of titanium 1.50 and 2.00 (wt %) showed lower pH values which might have delayed the release of alkaline ions form the glass. It was reported that the transition metal ions in 1393 bioactive glasses often showed a largely controllable dissolution properties within physiological fluids and their exciting route for potential delivery systems within tissue regeneration scaffolds.

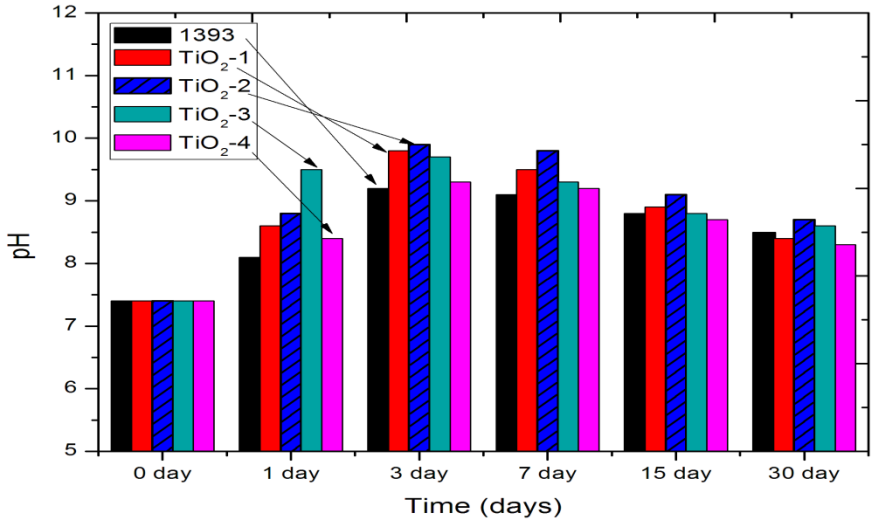

Fig 3:- pH 1393 and titanium oxide doped bioactive glass.

In Vitro bioactivity of 1393 and doped bioactive glass by Reflection spectroscopy:-

Fig: - 4, 5, 6, & 7 show the FTIR Reflection spectra bands of the bioactive glass before and after immersion in SBF for different days 0, 1, 3,7,15 and 30. Hench et al., 1998; Kim et al., 2000 and filgueira et al., 2002 demonstrated that effect in the IR spectra bands after immersion in SBF for protracted time period and the stages of apatite formation on the surface of the samples after immersion in SBF.

Fig: - 4 shows the IR spectra bands of TiO_2-1 sample before and after treated with SBF. The new bands were appeared after 1 day immersion in SBF when compared to before immersion at 596 and 690 cm^{-1} are corresponds to P–O bending (crystalline) and P–O bending (amorphous) bending respectively presence of C-O stretching 880cm^{-1} bond show the crystalline nature indicates the formation of hydroxyl carbonate apatite(HCA) layer. The bands at about 1431 and 1588 cm^{-1} are associated with C-O (Stretch) and C=O (Stretch) stretching mode and the broad band at about 3772 cm^{-1} can be assigned to (hydroxyl) O-H groups on the surface The protracted period of the samples in SBF shows the same behavior with small decrease in the intensities of the bands, which resulted in the formation of hydroxyl carbonated apatite (HCA) layer.

Fig: - 5 shows the IR spectra bands of TiO_2-2 sample before and after treated with SBF. The new bands were appeared after 1 day immersion in SBF when compared to before immersion at 534 and 612 cm^{-1} are corresponds to P–O bending (crystalline) and P–O bending (amorphous) bending respectively presence of C-O stretching 880 cm^{-1} bond show the crystalline nature indicates the formation of hydroxyl carbonate apatite(HCA) layer. The bands at about 1430 and 1589 cm^{-1} are associated with C-O (Stretch) and C=O (Stretch) stretching mode and the broad band at about 3773 cm^{-1} can be assigned to (hydroxyl) O-H groups on the surface The protracted period of the samples in

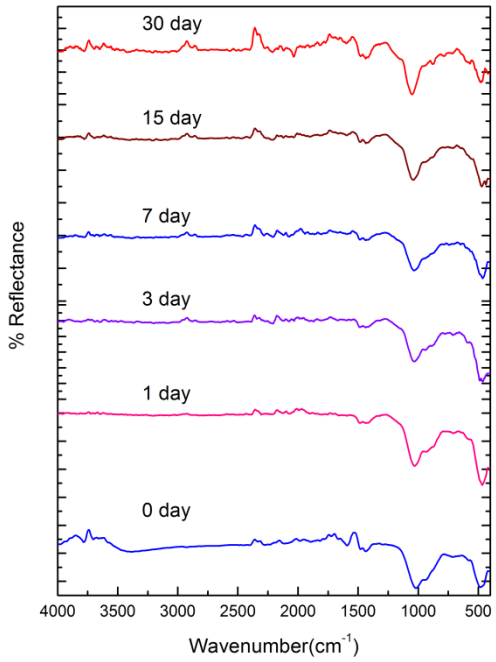

Fig 4:- FTIR reflectance spectra of TiO_2-1

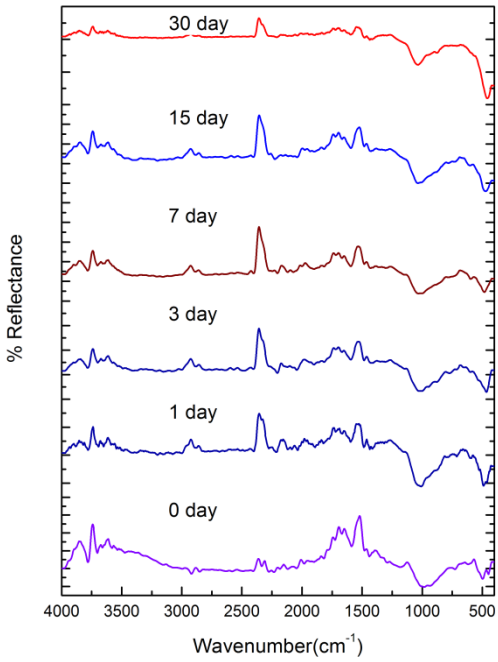

Fig 5:- FTIR reflectance spectra of TiO_2-2

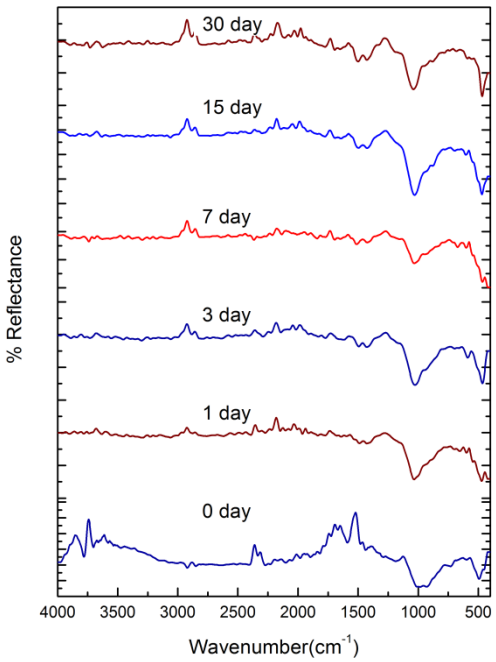

Fig 6:- FTIR reflectance spectra of TiO_2-3

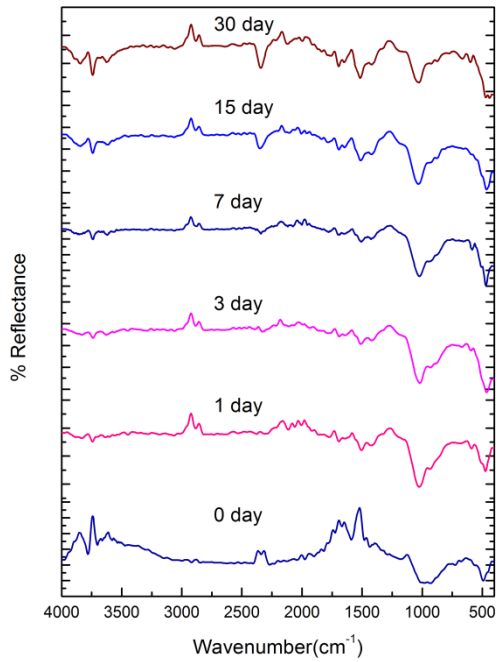

Fig 7:- FTIR reflectance spectra of TiO_2-4

SBF shows the same trend with small decrease in the intensities of the bands, which are resulted in favor of development of hydroxyl carbonated apatite (HCA) layer.

]

Fig:- 6 shows the IR spectra bands of TiO_3-3 sample before and after treated with SBF. The new bands were appeared after 1 day immersion in SBF when compared to before immersion at 581 and 659 cm^{-1} are corresponds to P–O bending (crystalline) and P–O bending (amorphous) bending respectively presence of C-O stretching 862 cm^{-1} bond show the crystalline nature indicates the development of hydroxyl carbonate apatite(HCA) layer. The bands at about 1414 and 1588 cm^{-1} are associated with C-O (Stretch) and C=O (Stretch) stretching mode and the broad band

at about 3774 cm^{-1} can be assigned to (hydroxyl) O-H groups on the fine surface The protracted period of the samples in SBF shows the same behavior with small decrease in the intensities of the bands, which are resulted in favor of development of hydroxyl carbonated apatite (HCA) layer.

Fig:- 7 shows the IR spectra bands of TiO_4-4 sample before and after treated with SBF. The new bands were appeared after 1 day immersion in SBF when compared to before immersion at 565 and 559 cm^{-1} are corresponds to P–O bending (crystalline) and P–O bending (amorphous) bending respectively presence of C-O stretching 927 cm^{-1} bond show the crystalline nature indicates the development of hydroxyl carbonate apatite(HCA) layer. The bands at about 1494 and 1603 cm^{-1} are associated with C-O (Stretch) and C=O (Stretch) stretching mode and the broad band at about 3775 cm^{-1} can be assigned to (hydroxyl) O-H groups on the surface The prolonged period of the samples in SBF shows the same behavior with small decrease in the intensities of the bands, which are resulted in favor of development of hydroxyl carbonated apatite (HCA) layer.

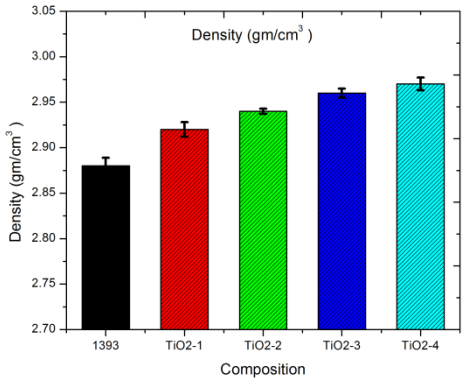

Fig 8:- Density of bioactive glass

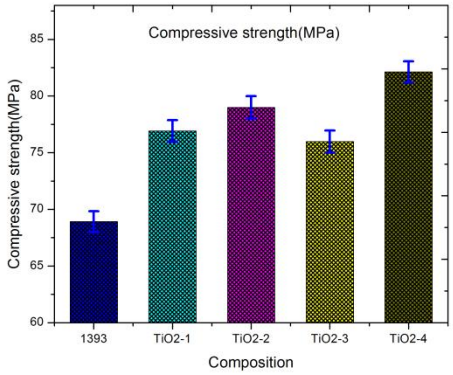

Fig 9:- Compressive strength of glass

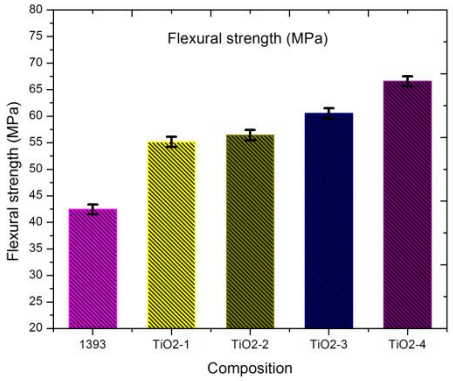

Fig 10:- Flexural strength of bioactive glass

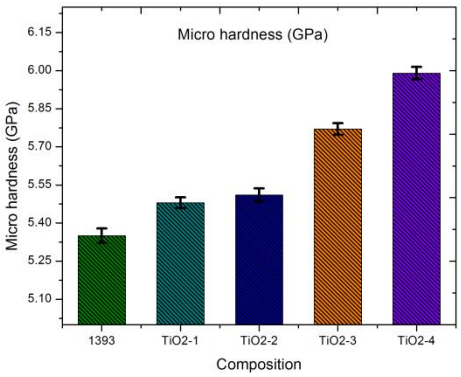

Fig 11:- Micro hardness of glass.

Mechanical behavior 1393 and doped bioactive glass:-

Fig:- 8 show the density of titanium oxide doped 1393 bioactive glass. It is observed that the densities of the samples were increased with increasing titanium oxide content from 2.76 to 2.86 gm/cm^3, which may be due to partial replacement of SiO_2 with TiO_2, and is attributed due to the replacement of a light element (density of SiO_2 - 2.64) with a heavier one (TiO_2 4.23). A similar trend of results also found in the compressive strength (1393, TiO_2-1 TiO_2-2, TiO_2-3 and TiO_2-4 and 67.62, 75.82, 76.62, 77.78 and 81.11 MPa respectively) shown in **Fig: - 9**.

Fig:- 10 and 11 shows the results of the flexural strength and Micro hardness of 1393, TiO_2-1, TiO_2-2, TiO_2-3 and TiO_2-4 samples. The results demonstrate an increasing tendency in flexural strength and Micro hardness as the percentage of titanium oxide (43.36, 54.75, 56.32, 59.22 and 63.42 Micro hardness 5.25, 5.38, 5.41, 5.57 and 5.69 respectively). This increase may be due to the Ti^{2+} may act as network intermediate, thus more the compactness of glass structure (Gehan et al., 2009). Vyas et. al., 2015 in an earlier investigation had also shown that the addition of cobalt oxide up to 2.0 wt% in 45S5 glass & glass-ceramic has resulted in an increase in density and compressive strength, flexural strength and Micro hardness.

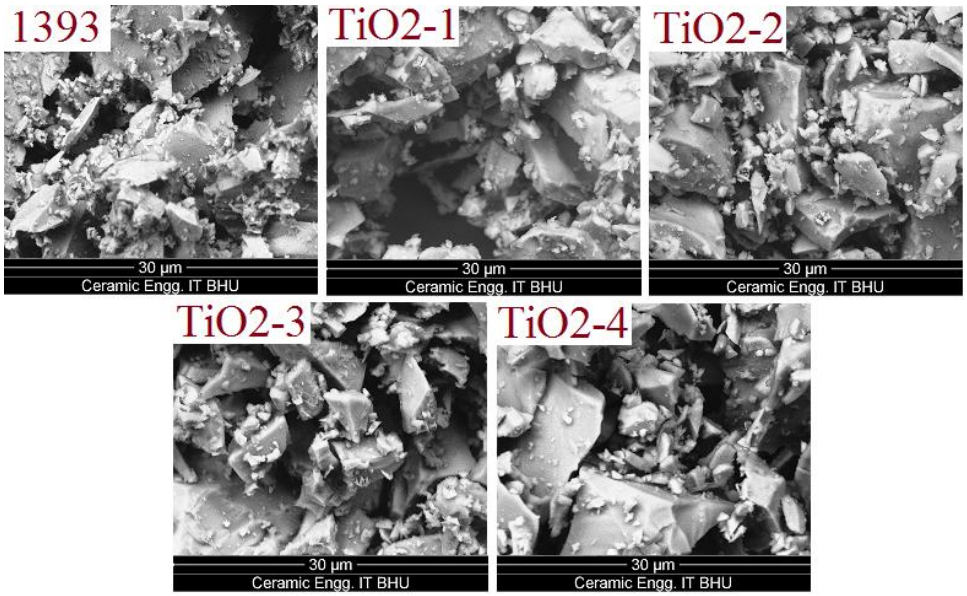

Fig 12:- Scanning Electron Microscope (SEM) of bioactive glasses before immersion in SBF for 7 days

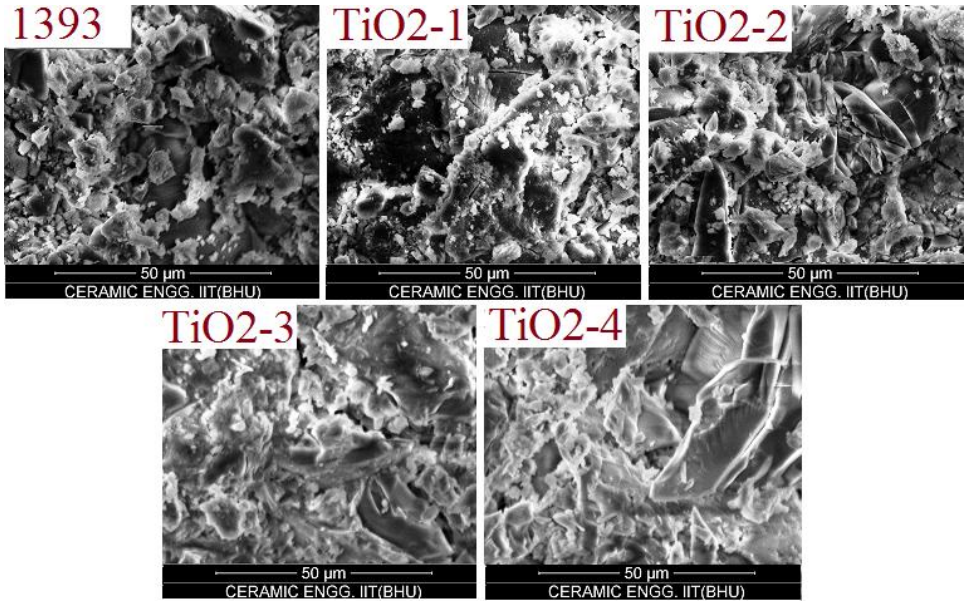

Fig 13:- Scanning Electron Microscope (SEM) of bioactive glasses after immersion in SBF for 7 days

Scanning Electron Microscopy (SEM):-

The SEM micrographs of 1393 glass and titanium oxide doped glass samples before immerse in SBF solution are shown in **Fig:- 12** which results in different rod types of structure and asymmetrical grain of 1393 bioactive glass samples and is quite similar to the results reported by (Hanan et al.,2009). **Fig: - 13** represent the SEM micrographs of base glass and titanium oxide doped bioactive glass of after immersed in SBF solution for 7 days. It is understandable from the **Fig: -13** that base and bioactive doped glass samples which were immersed in SBF solution for 7 days were enclosed with asymmetrical shape and grounded HA particles have been grown into more than a few agglomerates consisting of spine shaped HA layer. These micrographs show the formation of HA on the surface of the base and 1393 bioactive doped glass samples after immersion in SBF solution for 7 days (Tadashi et al., 2003).

Conclusions:-

In the present investigation, a comparative investigation was made on physico-mechanical and bioactive properties of titanium oxide doped 1393 bioactive glasses. The following conclusions were drawn from this investigation. It is concluded that an increase in titanium oxide content in this series of glasses resulted in an increase in bioactivity. This is also supported by pH and SEM analysis. FTIR results showed the silicate network structure in prepared bioactive glass and increasing the titanium oxide content in 1393 bioactive glass increase the density, flexural strength, compressive strength and micro hardness.

Acknowledgement:-

The authors gratefully acknowledge the HOD, Department of Ceramic Engineering, Indian Institute of Technology (Banaras Hindu University) Varanasi -221005, India the honorable Director of Indian Institute of Technology (Banaras Hindu University) Varanasi, India for providing necessary facilities for the present work.

Reference:-

1. **D.-M. Liu. (1994).** Mater. Chem. Phys. 36: (3–4) 294.
2. **L.L. Hench. (1991).** J. Am. Ceram. Soc. 74:1487.
3. **B.E. Buck, T.I. Malinin and M.D. (1989).** BrownClin. Orthop. 240:129.
4. **Hench, L.L., Wilson, J. (1993).** An Introduction to Bioceramics (Singapore: World Scientific Publishing Co. Pte. Ltd.) p 47.
5. **Hench, L.L. (2006).** The story of bioactive glass. J Mater Sci: Mater Med. 17, 967–978.
6. **Hench LL, Splinter, R. J., Allen, W. C. and Greenlee. (1971).** T. K. Bonding mechanisms at the interface of ceramic prosthetic materials. Journal of Biomedical Materials Research Symposium; 5:25.
7. **K. Franks, I. Abrahams, G. Georgiou, J.C. Knowles.(2001).** Biomaterials, 22, p. 497
8. **V. Patricia, M.P. Marivalda, M.G. Alfredo, L. Fatima. (2004).**Biomaterials, 25, p. 2941.
9. **Oana Bretcanu et al. (2009).** Journal of the European Ceramic Society 29 ,3299–3306.
10. **M.H. Fathi, A. Hanifi. (2007).** Evaluation and characterization of nanostructure hydroxyapatitepowder prepared by simple sol–gel method, Mater. Lett. 61, 3978–3983.
11. **I. Kansal, A. Goel, D.U. Tulyaganov, L.F. Santos, J.M.F. Ferreira.(2011).** Structure, surface reactivity and physico-chemical degradation of fluoride containing phospho-silicateglasses, J. Mater. Chem. 21 (22) 8074–8084.
12. **T. Kokubo, H.-M. Kim, M. Kawashita.(2003).** Novel bioactive materials with different mechanicalproperties, Biomaterials 24, 2161–2175.
13. **D. Shim, D.S.Wechsler, T.R. Lloyd, R.H. Beekman. (1996).** Hemolysis following coil embolization of a patent ductus arteriosus, Catheter. Cardiovasc. Diagn. 39 (3) 287–290.
14. **S.J.Watts, R.G. Hill,M.D. O'Donnell, R.V. Law. (2010).** Influence ofmagnesia on the structure and properties of bioactive glasses, J. Non-Cryst. Solids 356 (9–10) 517–524.
15. **K. Rezwan, Q.Z. Chen, J.J. Blaker, A.R. Boccaccini. (2006).** Biodegradable and bioactive porous polymer/inorganic composite scaffolds for bone tissue engineering, Biomaterials 27 (18) 3413–3431.
16. **C. Austin, T.M. Smith, A. Bradman, K. Hinde, R. Joannes-Boyau, D. Bishop, D.J. Hare, P.Doble, et al. (2013).** Barium distributions in teeth reveal early-life dietary transitions in primates, Nature 498 (7453) 216–219.
17. **G. Kaur, P. Sharma, V. Kumar, K. Singh. (2012).** Assessment of in vitro bioactivity of SiO2– BaO–ZnO–B2O3–Al2O3 glasses: an optico-analytical approach, Mater. Sci. Eng. C 32 (7) 1941–1947.
18. **W. Leenakul, P. Kantha, N. Pisitpipathsin, G. Rujijanagul, S. Eitssayeam, K. Pengpat. (2013).** Structural and magnetic properties of SiO2–CaO–Na2O–P2O5 containing BaO–Fe2O3 glass–ceramics, J. Magn. Magn. Mater. 325 102–106.
19. **A.I. Vogel. (1969).**A Text-book of Quantitative Inorganic Analysis, Third edition The English Language Book Society, London, 472–473.
20. **T. Kokubo, H. Takadama. (2006).** How useful is SBF in predicting in vivo bone bioactivity? Biomaterials 27 (15) 2907–2915.
21. **P. Sooksaen, S. Suttiruengwong, K. Oniem, K. Ngamlamiad, J. Atireklapwarodom. (2008).** Fabrication of porous bioactive glass–ceramics via decomposition of natural fibres, J. Met. Mater. Miner. 18 (2) 85–91.
22. **S.M. Salman, S.N. Salama, H.a. Abo-Mosallam. (2012).** the role of strontium and potassium on crystallization and bioactivity of Na2O–CaO–P2O5–SiO2 glasses, Ceram. Int. 38 (1) 55–63.

23. **O. Bretcanu, X. Chatzistavrou, K. Paraskevopoulos, R. Conradt, I. Thompson, A.R. Boccaccini. (2009).** Sintering and crystallisation of 45S5 Bioglass® powder, J. Eur. Ceram. Soc. 29 (16) 3299–3306.
24. **O. Peitl Filho, G.P. LaTorre, L.L. Hench. (1996) .** Effect of crystallization on apatite-layer formation of bioactive glass 45S5, J. Biomed. Mater. Res. 30 (4) 509–514.
25. **V.R. Mastelaro, E.D. Zanotto, N. Lequeux, R. Cortes. (2000).** Relationship between shortrange order and ease of nucleation in Na2Ca2Si3O9, CaSiO3 and PbSiO3 glasses, J. Non-Cryst. Solids 262 (22) 191–199.
26. **C.Y. Kim, A.E. Clark, L.L. Hench. (1989).** Early stages of calcium-phosphate layer formation in bioglasses, J. Non-Cryst. Solids 113 (2) 195–202.
27. **H. ElBatal, M. Azooz, E.M. Khalil, A. Soltan Monem and Y. Hamdy.(2003).** Characterization of some bioglass–ceramics, Mater. Chem. Phys. 80 (3) 599–609.
28. **A.V. Gayathri Devi, V. Rajendran and N. Rajendran. (2010).** "Ultrasonic characterisation of calcium phosphate glasses and glass - ceramics with addition of TiO2", International Journal of Engineering Science and Technology vol. 2(6), pp. 2483-2490.
29. **A.V. Gayathri Devia ,V. Rajendran and N.Rajendranb.(2010).** Material Chemistry and Physics 124 ,312-318.
30. **J. P. Nayak, S. Kumar, and J. Bera. (2010).**Journal of Non-Crystalline Solids, 356, 1447–1451.
31. **Marta Cerrutia, David Greenspanb and Kevin Powers.(2005)**. Biomaterials 26,1665–1674.
32. **V.K.Vyas, A.Sampath Kumar, S.Prasad,S.P.Singh amd Ram Pyare. (2015).** Bull. Mater. Sci. @ Indian Academy of Sciences, Vol. 38, No. 4, pp. 957–964August.
33. **L.L. Hench. (1998).** Journal of American Ceramic Society 81 1705–1728.
34. **V.R.Mastelaro, E.D.Zanotto N.Lequeux and R.Cortes. (2000).** J.Non-Cryst. Solids 262 191–199.
35. **Rehman I, Karsh M, Hench LL and Bonfield W.(2000)**. J Biomed Mater Res. May;5(2):97-100.
36. **V.R.Mastelaro, E.D.Zanotto,N.Lequeux and R.Cortes. (2000).** J.Non-Cryst. Solids 262, 191–199.
37. **P. Ducheyne and Q. Qiu. (1999).** Biomaterials 20, 2287 – 2303.
38. **Hanan H. Beherei, Khaled R. Mohamed and Gehan T. El-Bassyouni. (2009).** Fabrication and characterization of bioactive glass (45S5)/titania biocomposites, Ceram. Int., 35, 1991-1997.